

Study of Critical Fluctuations in BaTiO₃ by Neutron Scattering†

Y. YAMADA* AND G. SHIRANE

Brookhaven National Laboratory, Upton, New York 11973

AND

A. LINZ

Center for Materials Science and Engineering, Massachusetts Institute of Technology,
Cambridge, Massachusetts 02139

(Received 20 June 1968)

Neutron scattering from BaTiO₃ crystal has been investigated in the critical region ($T_c=130^\circ\text{C}<T<270^\circ\text{C}$) above the ferroelectric Curie temperature. In this temperature range, strong quasi-elastic scattering was observed. The temperature dependence of the quasi-elastic scattering indicates that it is associated with a critical polarization fluctuation in the crystal. An energy analysis of the cross section proves that the polarization fluctuation in BaTiO₃ is of the relaxation type in this temperature region, with a relaxation time longer than 5×10^{-11} sec. This result is in marked contrast to the case of SrTiO₃ and KTaO₃. The neutron cross sections, observed as functions of temperature and wave number, can be interpreted equally well with either an overdamped phonon model or a tunneling-mode model. The strong anisotropy of the quasi-elastic scattering in reciprocal space indicates that the directions of strongest correlation of the fluctuation are along the (100) axes.

I. INTRODUCTION

IN recent years the mechanism of ferroelectric phase transition has been extensively reexamined from the viewpoint of lattice dynamics. This was initiated by theoretical studies of Anderson¹ and Cochran² in terms of a temperature-dependent low-frequency optical phonon. This soft-phonon mode theory is believed to be a particularly suitable explanation of ferroelectricity in the displacive-type ferroelectrics such as BaTiO₃. BaTiO₃ is the most extensively studied ferroelectric among the displacive-type ferroelectrics; in addition, it has the perovskite structure which is the simplest type to exhibit ferroelectricity. The name "displacive type" is used in contrast with another typical ferroelectric, namely, the order-disorder type represented by KH₂PO₄.

In the soft-phonon mode theory, it is assumed that the polarization fluctuations are entirely due to the excitation of optical lattice vibrations. In this case, the static dielectric constant is expressed in terms of the frequencies of the optical phonons as follows:

$$\epsilon(0)/\epsilon(\infty) = \prod_i \omega_{i\text{LO}}^2 / \prod_i \omega_{i\text{TO}}^2,$$

where $\epsilon(0)$ and $\epsilon(\infty)$ are the static and high frequency dielectric constants, and $\omega_{i\text{TO}}$ and $\omega_{i\text{LO}}$ are the characteristic frequencies of transverse and longitudinal optical modes. The dielectric anomaly near the critical temperature is connected to the temperature dependence of a particular transverse mode which has the form $\omega_i^2 \propto T - T_0$, with T_0 the paraelectric Curie temperature.

Experimentally, the existence of this soft-phonon mode and its strong temperature dependence have been observed in SrTiO₃ and KTaO₃. These are both perovskite-type crystals which show an anomalous temperature-dependent dielectric constant, but neither of these materials actually undergoes a ferroelectric transition. On the other hand, in the case of BaTiO₃, which undergoes a ferroelectric transition at 130°C, the results on the existence of a soft phonon mode as determined by different experimental techniques are found to be in disagreement with each other.

Infrared data have been analyzed by Barker³ using the classical oscillator model with a large damping force. At 200°C, the characteristic energy of the soft phonon mode $\hbar\omega_1$ was given as 5.2 meV (1 meV = 8.07 cm⁻¹), in agreement with Cochran's theory, along with a damping parameter of $\Gamma/2\omega_1 = 2$. On the other hand, Ballantyne⁴ found a dielectric loss peak at 1.6 meV at the same temperature. Recently, Harada *et al.*⁵ deduced a soft-phonon mode energy of 5.8 meV at $q = 0.34 \text{ \AA}^{-1}$ along [100] from x-ray diffuse scattering. The significance of this x-ray result is the fact that this optic mode energy lies below the energy of acoustic mode as determined by thermal neutrons (see Fig. 1).

The neutron scattering measurements⁶ are depicted in Fig. 1, which are in line with the x-ray result and Ballantyne's estimate at $q=0$. It was noted, however, that the cross section due to the excitation of this soft mode exhibited unusually weak intensities despite their low excitation energies.

It is the purpose of the present study to extend the neutron measurements into the important temperature

† Work performed under the auspices of the U. S. Atomic Energy Commission and Advanced Research Project Agency.

* On leave from Osaka University, Osaka, Japan.

¹ P. W. Anderson, in *Proceedings of the Conference on the Physics of Dielectrics*, edited by G. I. Skanavi (Academy of Science, Moscow, 1958), p. 290.

² W. Cochran, *Advan. Phys.* **9**, 387 (1960).

³ A. S. Barker, *Phys. Rev.* **145**, 391 (1966).

⁴ B. M. Ballantyne, *Phys. Rev.* **126**, 1710 (1962).

⁵ J. Harada, H. Motegi, G. Honjo, T. Mitsui, and S. Hoshino, *J. Phys. Soc. Japan* **22**, 1515 (1967).

⁶ G. Shirane, B. C. Frazer, V. J. Minkiewicz, J. A. Leake, and A. Linz, *Phys. Rev. Letters* **19**, 234 (1967).

range between the Curie temperature and 230°C. In particular, near the Curie temperature it is expected that the observation of the scattering due to polarization fluctuation will enhance our knowledge of the mechanism involved in the ferroelectric transition.

II. EXPERIMENTAL RESULTS

The measurements were performed at the Brookhaven high-flux beam reactor, utilizing a triple-axis spectrometer. The constant- Q technique⁷ was employed with a fixed incoming energy E_0 between 13 and 48 meV. A typical energy resolution was 0.70 meV FWHM (full width at half-maximum) at $E_0=17$ meV. This was obtained with 20-min collimator before and after the scattering and monochromator and analyzer crystals having mosaic spreads of approximately 15 min.

The BaTiO₃ single crystal utilized in the present investigation was the same sample used in the previous experiment,⁶ and the growth technique was described previously.⁸ It had a volume of 1.7 cm³ and an extremely narrow mosaic spread of less than 0.01°. The Curie temperature was determined as $(130 \pm 0.5)^\circ\text{C}$, on heating, by a discontinuous change of Bragg intensity. This crystal was indeed an excellent crystal and the only one available of this size. Unfortunately, however,

a few passages through the Curie temperature resulted in fracture of the crystal. Thus the present study was terminated somewhat prematurely.

The crystal was mounted with a $\langle 001 \rangle$ axis vertical. The momentum transfer $|\mathbf{q}|$ is expressed in units of \AA^{-1} , where the direction of \mathbf{q} is along $\langle 100 \rangle$ except when specified. The zone boundary value varies from 0.784\AA^{-1} to 0.783\AA^{-1} between 130°C and 270°C . The present experimental results may be divided into three categories according to the \mathbf{q} range. In order to specify the exact location of reciprocal space at which a cross section was measured, a coordinate of reciprocal space such as $(h+\xi, k+\eta, l+\zeta)$ is also used. In this expression, $(h+0.5, k, l)$ corresponds to the zone boundary along the $[100]$ direction around the reciprocal point (h, k, l) .

A. $q > 0.15 \text{\AA}^{-1}$

The results in this \mathbf{q} range were reported previously and are shown in Fig. 1. Since the data indicated only slight shift of energy between 430 and 230°C , no more effort was made to investigate this \mathbf{q} range at lower temperatures. As shown in Fig. 2(a), the main difficulty in observing the soft mode is its extremely weak intensity despite its low excitation energy. As a first approximation, let us assume that the inelastic scattering due to the soft mode and the TA mode has the same structure factors as those of the TO_1 and TA mode of

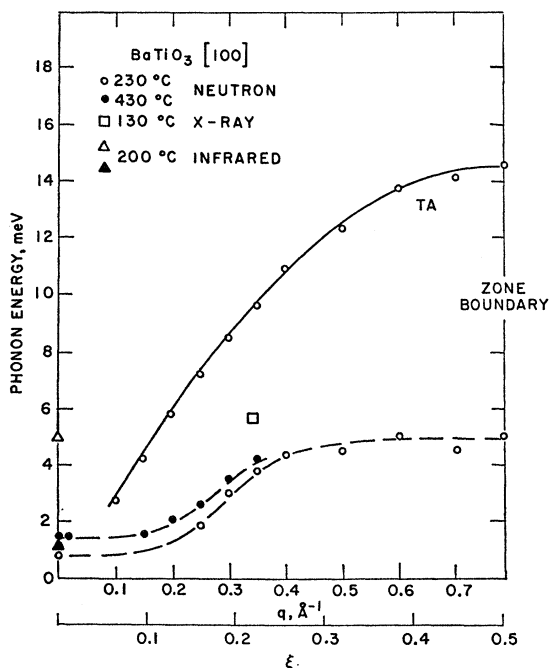


FIG. 1. Dispersion curves of BaTiO₃ in the paraelectric phase as determined by neutron scattering, along with the data given by various kinds of experiments hitherto available. References are given in the text.

⁷ B. N. Brockhouse, *Inelastic Scattering of Neutrons in Solids and Liquids* (International Atomic Energy Agency, Vienna, 1961).

⁸ A. Linz, V. Belruss, and C. S. Naiman, *J. Electrochem. Soc.* **112**, 60C (1965).

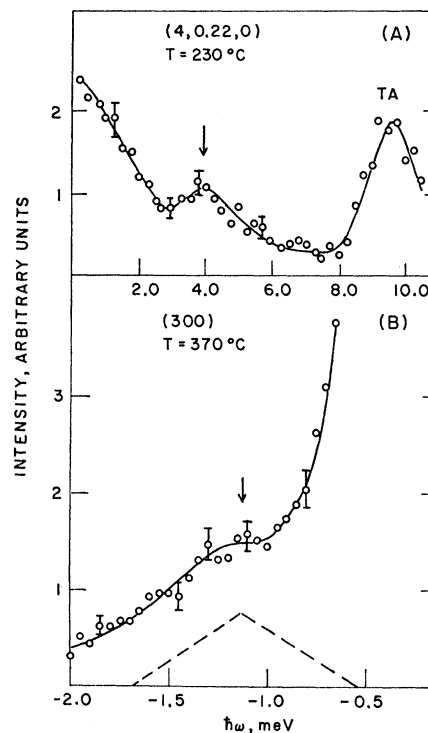


FIG. 2. Energy spectrum of neutron scattering at higher temperatures. Peaks indicated by arrows correspond to excitation of the low frequency mode. Positive values of $\hbar\omega$ correspond to neutron energy loss.

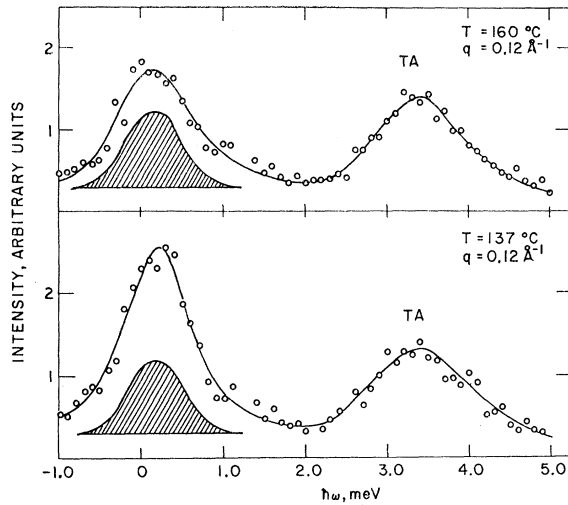


FIG. 3. Energy spectrum of neutron scattering at $(2,0,0.076,0)$. The shaded areas represent elastic scattering due to nuclear incoherent scattering.

SrTiO_3 . Following Cowley's⁹ calculation for SrTiO_3 , correcting for the mass difference of Ba and Sr, we have $|F_S|^2/|F_{TA}|^2=3.0$ around the $(4,0,0)$ reciprocal lattice point, where F_S and F_{TA} are the structure factors of the soft mode and TA mode, respectively. Therefore, the intensity ratio of the two peaks in Fig. 2(a) should

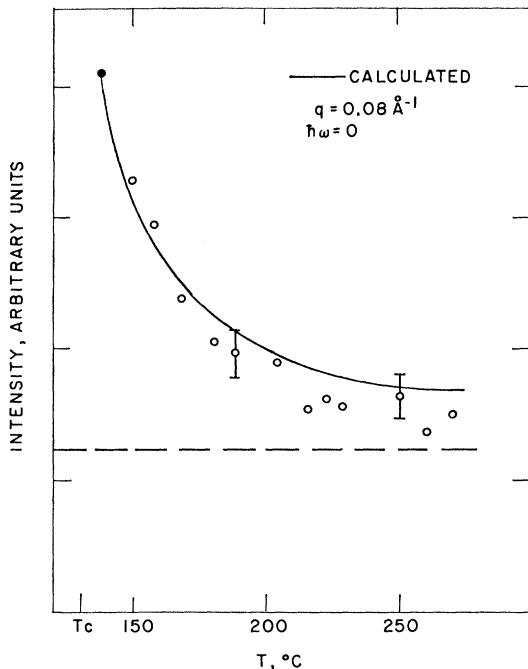


FIG. 4. Temperature dependence of the quasi-elastic scattering. The dashed line represents the temperature-independent cross section due to the nuclear incoherent scattering. The solid line is the calculated curve with Eq. (3), normalized at the point shown by the solid circle.

⁹ R. A. Cowley, Phys. Rev. **134A**, 981 (1964).

be approximately $|F_S|^2\omega_{TA}^2/|F_{TA}|^2\omega_S^2$. The observation indicates that the intensity due to the soft mode excitation is 60 times smaller than this ratio would indicate. This apparent intensity anomaly might be a result of an entirely different structure factor for BaTiO_3 compared with that for SrTiO_3 . In this case, one might expect stronger intensities in the vicinity of other types of reciprocal lattice points, such as $(1,0,0)$ and $(1,1,0)$. The measurements around $(3,0,0)$ and $(5,1,0)$ proved this is not the case.

B. $q < 0.05 \text{ \AA}^{-1}$

The measurement at $q=0$, with a resolution of 0.5 meV FWHM revealed a shoulder in energy spectrum as shown in Fig. 2(b). Compared with the resolution function (broken line), the profile does not appear very broad. It was reported previously⁶ that the energy of this peak decreases from 1.4 meV at 430°C to 0.8 MeV

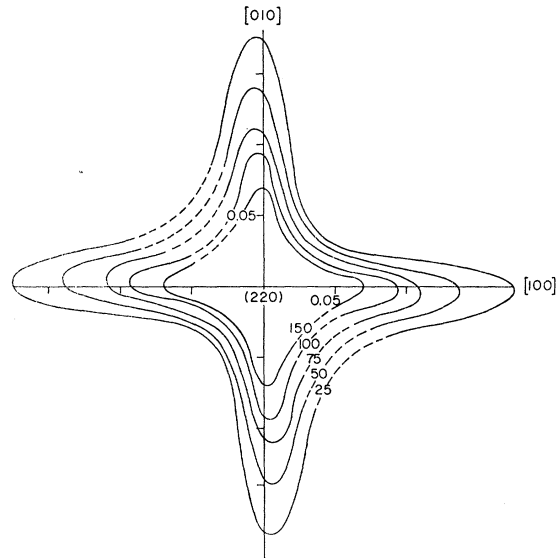


FIG. 5. Intensity distribution of the quasi-elastic scattering in q space around $(2,2,0)$. The dotted part is inaccurate because of the difficulty in subtracting the large background in the $[110]$ direction.

at 230°C . Below 230°C in the present investigation, the peak of the cross section at $q=0$ is extremely difficult to observe because of a large background due to low-energy phonons. Nevertheless, a slight shoulder around 1 meV seems to persist down to 137°C .

C. $0.05 \text{ \AA}^{-1} < q < 0.15 \text{ \AA}^{-1}$

This is the range of q where the peaks of the neutron scattering due to soft-mode excitation and TA-mode excitation come close together, and where the cross section due to soft-mode excitation was reported to be particularly small.⁶ In the present study, measurements were carried out mainly in this q range at temperatures

just above the Curie temperature. As is shown in Fig. 3, the inelastically scattered cross sections were not observed in this temperature range. Instead, a quasi-elastic scattering with an energy width less than 0.6 meV was observed. In this figure, the scattered neutron cross section at $(2,0.076,0)$ is plotted against the energy transfer, $\hbar\omega$, for the temperatures 137 and 160°C. The shaded part in the figure corresponds mostly to the elastic incoherent scattering due to the titanium and barium nuclei and was obtained by observing the cross section at $T=270^\circ\text{C}$. The width of this elastic peak therefore gives the instrumental energy resolution. In the figure, we clearly see the additional quasi-elastic scattering around $\hbar\omega=0$, rapidly increasing with decreasing temperature toward the Curie temperature. We call this quasi-elastic scattering "critical" scattering hereafter. The shift of the peak position from the zero energy value is caused by the combination of a strongly q -dependent critical scattering and the finite resolution of the neutron probe.

In Fig. 4, the observed temperature dependence of the quasi-elastic scattering cross section at $(2,2.05,0)$ is plotted. The temperature-independent component remaining above 250°C corresponds to the cross section due to the nuclear incoherent scattering mentioned above, and is indicated by the dashed line. The solid line corresponds to the calculated curve explained later. Here, it is emphasized that the observed intensity is considerably lower than calculated value at high temperatures.

It is of great interest to map out the intensity distribution in q space. The intensity distribution around (220) at $T=137^\circ\text{C}$ is given in Fig. 5. In the figure, we have subtracted the intensity distribution measured at $T=270^\circ\text{C}$ corresponding to the remanent background so that the contours show the distribution due to only the critical scattering. A marked elongation of the contour was observed along the $\langle 100 \rangle$ directions, which correspond to the direction perpendicular to polar axis of the tetragonal phase. This measurement was carried out in the Brillouin zone around (220) rather than (200) . This is due to a technical reason, namely, the resolution function of the neutron probe in reciprocal space is elongated along $[\bar{1}10]$ at $(2,2,0)$ and along $[010]$ at $(2,0,0)$.¹⁰ For this reason, the critical scattering in the $[010]$ direction about $(2,0,0)$, where the scattering is a maximum, would be superposed by an additional background of low-energy phonons. Around $(2,2,0)$, the added background is along $[\bar{1}10]$, where the critical scattering is a minimum; the dotted parts of the contours represent the parts where the additional background precluded an accurate measurement. The sections of the distribution along the $[010]$ direction at $T=137^\circ\text{C}$ and $T=270^\circ\text{C}$ are plotted in Fig. 6.

The results of the energy analysis at $q=0.08 \text{ \AA}^{-1}$, 0.12 \AA^{-1} , and 0.16 \AA^{-1} are shown in Fig. 7. The increase

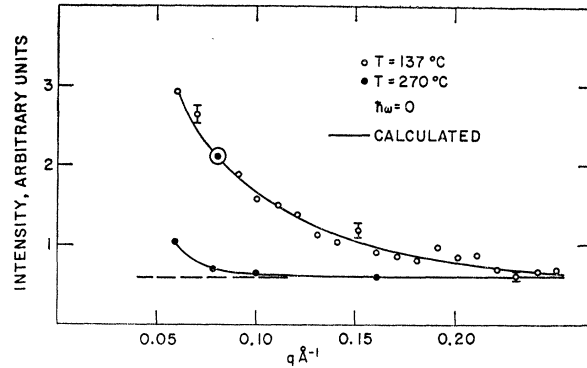


FIG. 6. Wave number dependence of the quasi-elastic scattering along the $[010]$ direction at $T=137^\circ\text{C}$ and $T=270^\circ\text{C}$. The solid line for $T=137^\circ\text{C}$ represents the calculated curve with Eq. (3), normalized at the point shown by the double circle.

of intensities for $|\hbar\omega| \geq 1.0$ meV in the profile of $q = 0.08 \text{ \AA}^{-1}$ is due to the finite resolution detecting the excitation and the deexcitation of transverse acoustic phonons.

III. ANALYSIS OF CRITICAL SCATTERING

The q dependence and the temperature dependence of the quasi-elastic scattering are similar to the critical scattering which is observed in magnetic substances near the magnetic transition point, as well as in other substances which undergo various kinds of order-dis-

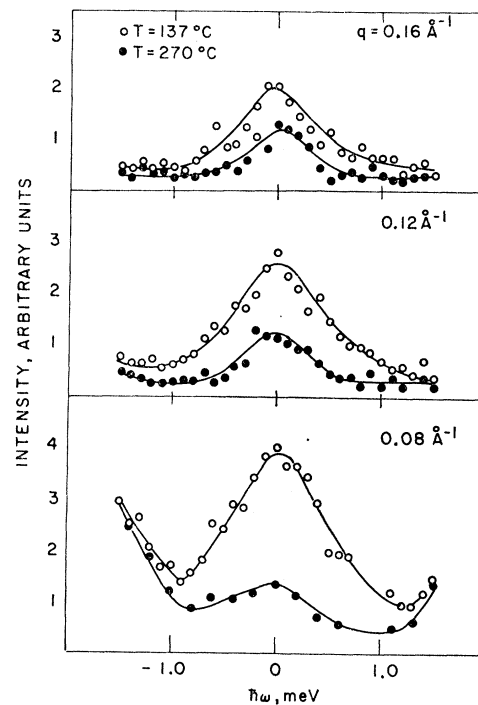


FIG. 7. Energy spectrum of the quasi-elastic scattering at three values of q taken along the $[010]$ direction. Curves with black circles taken at $T=270^\circ\text{C}$ corresponds to the cross section without critical scattering.

¹⁰ M. J. Cooper and R. Nathans, *Acta Cryst.* **23**, 357 (1967).

order phase transitions. Therefore, it is inferred that the observed quasi-elastic scattering of neutrons in BaTiO₃ is directly connected to large fluctuations of the atomic positions near the critical point which is accompanied by the polarization fluctuation.

Van Hove¹¹ has shown that the neutron-scattering cross section due to the particle-density fluctuation near the critical point is given by

$$\frac{d^2\sigma}{d\Omega d\omega} = \text{const} \frac{1}{\kappa^2 + q^2} \frac{\gamma}{\omega^2 + \gamma^2}, \quad (1)$$

where the reciprocal of γ is the relaxation time of the time-dependent fluctuation, while the reciprocal of κ is called correlation length of the fluctuation and varies with temperature as $(T - T_c)^\nu$, ν being a number of order of 1. As is discussed later, in the case of BaTiO₃, where the static dielectric susceptibility obeys the Curie-Weiss law over the temperature range under investigation, we may take ν as $\frac{1}{2}$, or

$$\kappa^2 = A(T - T_0). \quad (2)$$

T_0 is the paraelectric Curie temperature and A is a parameter to be determined by the experiment. Substitution of (2) into (1) gives

$$\frac{d^2\sigma}{d\Omega d\omega} = \text{const} \frac{1}{A(T - T_0) + q^2} \frac{\gamma}{\omega^2 + \gamma^2}, \quad (3)$$

which will be used to analyze our results.

A. ω Dependence

The value of γ is estimated from the line shape of the inelasticity of the quasi-elastic scattering. The instrumental energy resolution function was approximated by the elastic peak observed at 270°C. It can be expressed by a Gaussian distribution function with 0.72 ± 0.15 meV FWHM. According to Eq. (3), the ω dependence of the critical scattering is given by a Lorentzian distribution. To obtain the value of γ , we fold a Lorentzian function with the Gaussian resolution function. The folded curves are compared with the experimental line shapes to determine the parameter γ of the Lorentzian function. The estimated inelasticity for various \mathbf{q} values and temperatures are summarized as follows. Data taken around (2,2,0) reciprocal lattice point at $T = 137^\circ\text{C}$ give the value of $\hbar\gamma$ as 0.40 ± 0.15 , 0.55 ± 0.15 , and 0.60 ± 0.15 meV for $q = 0.08 \text{ \AA}^{-1}$, 0.12 \AA^{-1} , and 0.16 \AA^{-1} , respectively. Data taken around (2,0,0) at $q = 0.12 \text{ \AA}^{-1}$ give 0.35 ± 0.15 and 0.35 ± 0.15 meV at $T = 137$ and 160°C , respectively. The energy width of the observed critical scattering changes appreciably in the process of subtracting the incoherent scattering, which introduces a large uncertainty of ± 0.15 meV. Within this error we could observe neither appreciable q dependence nor temperature dependence in γ .

¹¹ L. Van Hove, Phys. Rev. **95**, 249 (1954).

B. Correlation Length

In Eq. (3), A and T_0 are considered parameters to be determined so that a best fit with the experimental curves shown in Figs. 4 and 6 is attained. To obtain these parameters we proceed as follows. We plot the temperature dependence of the inverse of the relative intensity, $1/I$ at $q = 0.08 \text{ \AA}^{-1}$ and the q dependence of $1/I$ along $[\xi 00]$ at $T = 137^\circ\text{C}$, which gives

$$\begin{aligned} \text{at } q = q_1: & \quad 1/I \propto (T - T_0) + \Delta T, \quad \Delta T = q_1^2/A, \\ \text{at } T = T_1: & \quad 1/I \propto \kappa^2 + q^2, \quad \kappa^2 = A(T_1 - T_0). \end{aligned}$$

The extrapolation of the observed curves gives

$$\begin{aligned} \Delta T = T_0 - 110^\circ\text{C} & \quad \text{at } q_1 = 0.08 \text{ \AA}^{-1}, \\ \kappa^2 = 0.0055 \text{ \AA}^{-2} & \quad \text{at } T_1 = 137^\circ\text{C}, \end{aligned}$$

whence the parameters are determined as

$$\begin{aligned} T_0 &= 124^\circ\text{C}, \\ A &= 0.43 \times 10^{-2} \text{ \AA}^{-2} \text{ deg}^{-1}. \end{aligned}$$

The difference of the paraelectric Curie temperature and the observed transition temperature, $T_c - T_0$, is 6°C . The same quantity given by Roberts¹² from a measurement of the dielectric constant is 12°C .

C. Absolute Value of the Integrated Intensity

The data shown in Fig. 7 also give us an estimate of the absolute value of the critical scattering cross section integrated through ω . The temperature-independent part of the elastic peak observed at 270°C is due to the nuclear incoherent scattering.

In such circumstances, we obtain the absolute value of the differential cross section of the critical scattering from the following equation:

$$\left(\frac{d\sigma}{d\Omega} \right)_{\text{orit}} = \frac{I_{\text{orit}} \sigma_{\text{inc}}}{I_{\text{inc}} 4\pi}, \quad (4)$$

where σ_{inc} (5.6 b/sr) is the total incoherent-scattering cross section, I_{orit} and I_{inc} are the observed scattered intensities of the critical scattering and the incoherent scattering, respectively. The observed value is

$$(d\sigma/d\Omega)_{\text{orit}} = 1.51 \text{ b/sr} \quad (5)$$

for $T = 137^\circ\text{C}$ and $q = 0.12 \text{ \AA}^{-1}$.

IV. MODELS

To interpret the experimental results mentioned above, we set up models describing the dynamical behavior of the atoms in BaTiO₃.

A. "Harmonic Oscillator" Model

One possible interpretation might be to assume that the observed peak is the overlap of two peaks due to the

¹² S. Roberts, Phys. Rev. **75**, 989 (1949).

excitation and deexcitation of a very soft mode with phonon energy less than the resolution function ($\hbar\omega \leq 0.6$ meV). However, this possibility is ruled out by the following reason. The integrated scattering cross section due to one-phonon excitation or deexcitation is given by

$$\left(\frac{d\sigma}{d\Omega}\right)_{\text{ph}} = N \frac{k'}{k} \frac{\hbar}{2\omega} |F_{\text{ph}}(\mathbf{K})|^2 \frac{kT}{\hbar\omega}. \quad (6)$$

Here, N is the number of the unit cells and the phonon excitation number is approximated by $kT/\hbar\omega$. $F_{\text{ph}}(\mathbf{K})$ is the structure factor given explicitly by

$$F_{\text{ph}}(\mathbf{K}) = \sum_j (\mathbf{K} \cdot \mathbf{e}_j) \frac{b_j}{\sqrt{M_j}} e^{i\mathbf{K} \cdot \mathbf{r}_j}, \quad (7)$$

where \mathbf{e}_j is the polarization vector, M_j is the mass, b_j is the nuclear scattering amplitude, and \mathbf{r}_j is the position vector of j th atom in the unit cell, respectively. Assuming the polarization vector for this mode to be the same as the soft mode in SrTiO₃ (Ti: 0.077, Sr: 0.022, O_I and O_{II}: -0.129, O_{III}: -0.093), we calculate the integrated scattering cross section at (220) as

$$(d\sigma/d\Omega)_{\text{ph}} = 170 \text{ b/sr}.$$

This is larger than the observed intensity at (2,2.05,0) at $T=137^\circ\text{C}$ by a factor of 10^2 .

B. "Overdamped" Phonon Model

In the case of the harmonic phonon, the peak position of the neutron inelastic scattering directly corresponds to the phonon energy. However, if the phonon system is affected by large damping due to the anharmonicity, this is no longer satisfied. The nature of the response of such an anharmonic crystal to neutron waves was studied by Cowley¹³; he gave an explicit expression for the damping constant in terms of the third- and the fourth-order anharmonic potential. However, we might not be able to apply his results because these formulas are based on a perturbation treatment assuming the anharmonic interaction is small compared with the harmonic interaction, which is not valid in our case. Therefore, we might satisfy ourselves by using a somewhat phenomenological treatment, in which the anharmonic effect is expressed by a frequency-dependent damping parameter in the equation describing the motion of phonon operator. The calculation to obtain the neutron scattering cross section from such a system has been performed by Blume.¹⁴ The result is

$$\left(\frac{d^2\sigma}{d\Omega d\omega}\right)_{\text{ph}} = N \frac{k'}{k} |F_{\text{ph}}(\mathbf{K})|^2 \frac{kT}{\pi \hbar} \times \frac{\Gamma'(\mathbf{q},\omega)}{(\omega_1^2 - \omega^2 - \omega\Gamma''(\mathbf{q},\omega))^2 + \omega^2\Gamma'^2(\mathbf{q},\omega)}, \quad (8)$$

¹³ R. A. Cowley, *Advan. Phys.* **12**, 421 (1963).

¹⁴ M. Blume (private communication).

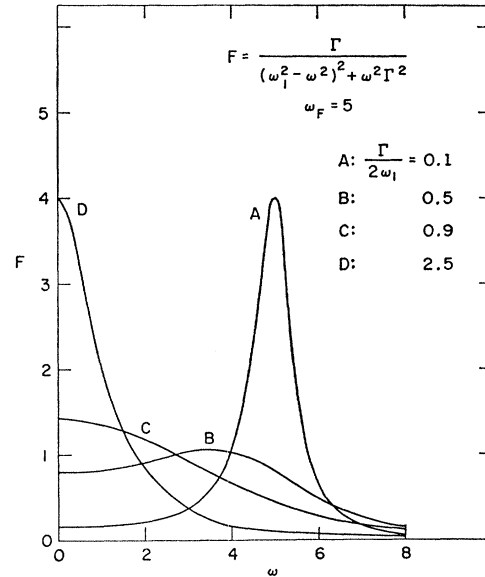


FIG. 8. Calculated curves for line profile of neutron scattering due to damped phonon. Observed line profile corresponds to the case D, highly overdamped case.

where $\Gamma'(\mathbf{q},\omega)$ and $\Gamma''(\mathbf{q},\omega)$ are the real and the imaginary parts of $\Gamma(\mathbf{q},\omega)$, respectively.

Barker³ and DiDomenico *et al.*¹⁵ have derived essentially equivalent formulas to explain infrared and Raman spectra, respectively, in BaTiO₃. As is discussed by these authors, when the damping constant exceeds $\sqrt{2}\omega_1(\mathbf{q})$ the motion of the soft mode is simply of the relaxation type. This situation is illustrated in Fig. 8 for the simple case where $\Gamma''=0$, and Γ' is independent of ω . In the figure, the line profiles are shown for several values of $\Gamma'/2\omega_1$. For $\Gamma'/2\omega_1 \gg 1$, as in case D, the line shape is sharply peaked at $\omega=0$. The observed neutron scattering cross section has the characteristic of case D. In this case, it is not possible to determine uniquely ω_1 and Γ' from the experimental line shape. In fact, for sufficiently large $\Gamma'/2\omega_1$, we can rewrite the formula as follows:

$$\left(\frac{d^2\sigma}{d\Omega d\omega}\right)_{\text{sp}} \cong N \frac{k'}{k} |F_{\text{ph}}(\mathbf{K})|^2 \frac{\hbar kT}{\pi} \frac{1}{(\hbar\omega_1)^2} \frac{\omega_1^2/\Gamma'}{\omega^2 + (\omega_1^2/\Gamma')^2}. \quad (9)$$

The line profile is given by a Lorentzian as is predicted in Eq. (3), and the half-width is ω_1^2/Γ' . To visualize further the close relation between Eqs. (3) and (9), we may expand the undamped soft-mode frequency $\omega_1(\mathbf{q})$ as $[\hbar\omega_1(\mathbf{q})]^2 \cong [\hbar\omega_1(0)]^2 + a\mathbf{q}^2$. Since the static dielectric susceptibility due to the soft mode is proportional to $1/\omega_1^2(0)$, and the temperature dependence of the static dielectric susceptibility obeys the Curie-Weiss law in the temperature region under investigation, we may put

$$[\hbar\omega_1(0)]^2 = \alpha(T - T_0),$$

¹⁵ M. DiDomenico, Jr., S. P. S. Porto, and S. H. Wemple, *Phys. Rev. Letters* **19**, 855 (1967).

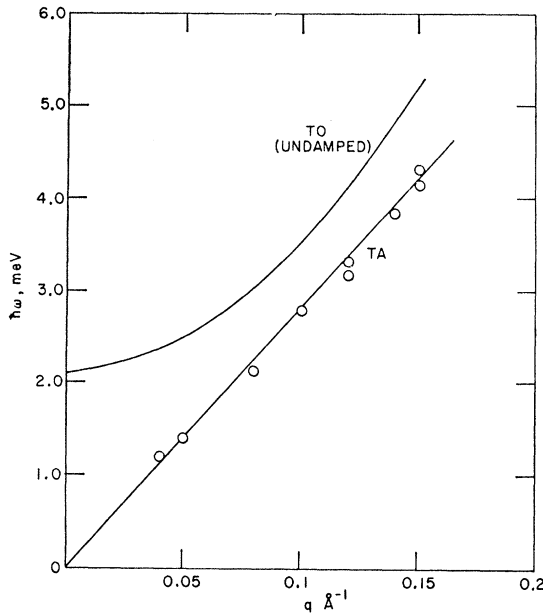


FIG. 9. Dispersion curve for quasi-harmonic (undamped) TO mode at $T=137^\circ\text{C}$. Because of high damping constant the peak of the neutron scattering is at $\hbar\omega_1=0$. The dispersion for TA branch is also shown. The initial slope calculated with the elastic constant is shown by the solid line.

assuming that the frequencies of the other optical phonons are temperature-independent. With these equations, we have

$$\left(\frac{d^2\sigma}{d\Omega d\omega}\right)_{dp} \cong N \frac{k'}{k} |F_{\text{ph}}(\mathbf{K})|^2 \frac{\hbar k T}{\pi} \frac{1}{\alpha(T-T_0) + aq^2} \times \frac{\omega_1^2/\Gamma'}{\omega^2 + (\omega_1^2/\Gamma')^2}. \quad (10)$$

This formula coincides with Eq. (3) if we equate

$$A = \alpha/a, \quad \gamma = \omega_1^2/\Gamma'.$$

To obtain ω_1 and Γ' separately from the observed value of A and γ , we have to determine α . Barker³ determined the parameter α as $0.28 \text{ meV}^2 \text{ deg}^{-1}$, using the Lyddane-Sachs-Teller relation and the frequencies of the optical modes determined from the infrared spectra. With this value of α we can obtain $\omega_1(\mathbf{q})$ for small values of \mathbf{q} . The dispersion curve for $0 \leq \xi \leq 0.10$ at 137°C thus determined is shown in Fig. 9. It should be noted that although the peak of the neutron scattering due to the soft-mode excitation comes below the dispersion curve of the TA mode even at higher temperatures, the dispersion curve of the undamped mode lies above that of the TA mode. If, however, this value of α is to be modified because of the contribution to the dielectric constant from an additional degree of freedom which is related to an optical-type displacement of atoms, then the whole curve should be shifted accordingly. From the

calculated values of γ and $\omega_1(\mathbf{q})$ given above, we obtain a very high damping parameter ($\Gamma'/2\omega_1$) (which corresponds to Γ used by DiDomenico *et al.*¹⁵).

$$\Gamma'/2\omega_1 = 4.6_{-1.5}^{+5}$$

at $T=137^\circ\text{C}$ and $q=0.12 \text{ \AA}^{-1}$.

Another way to determine $\omega_1(\mathbf{q})$ uniquely is to utilize the expression for the absolute integrated intensity:

$$(d\sigma/d\Omega)_{dp} = N(k'/k) |F_{\text{ph}}(\mathbf{K})|^2 (kT/\omega_1^2(\mathbf{q})). \quad (11)$$

The observed intensity was scaled in an absolute manner by comparison with the incoherent scattering at $T=137^\circ\text{C}$ and $q=0.12 \text{ \AA}^{-1}$. The energy $\hbar\omega_1(\mathbf{q})$ was calculated as $\hbar\omega \cong 3.4 \text{ meV}$. From Fig. 9, we see $\hbar\omega_1(\mathbf{q}) = 4.2 \text{ meV}$. This process of arriving at the phonon frequency involves the assumption of the form factor. In this calculation, we applied the same form factor used in the harmonic model; thus the order of magnitude agreement could be fortuitous.

C. "Tunneling Mode" Model

In this model, we assume that the atoms are tunneling through a potential barrier between equilibrium positions displaced by a certain amount, Δr_j for the j th atom, from the position of the center of symmetry. Such a model has been discussed by several authors to explain the ferroelectric transition in KH_2PO_4 .¹⁶⁻²⁰ BaTiO_3 is usually considered to be a typical displacive-type ferroelectric in which the polarization fluctuation is described by the excitation of an optical phonon mode and where the dynamical behavior of the atoms is quite different from the order-disorder-type ferroelectrics such as KH_2PO_4 . However, a few years ago, Takahashi²¹ pointed out that the polarization fluctuation in BaTiO_3 may not be described by a phonon picture because of the large anharmonicity, but rather can be described by another kind of motion in which the atoms are jumping from one extreme position to another. His picture seems to be similar to the model presented in this section.

In the case of KH_2PO_4 , each hydrogen atom is moving between two potential minima. According to Tokunaga and Matsubara,¹⁷ such a system can be treated as an Ising spin system with spin quantum number $\frac{1}{2}$. The eigenstates of the fictitious spin would correspond to the states where atoms are moving around one of the double minima of the potential. Since BaTiO_3 has a high-crystal symmetry, there are six positions of the potential minima (two on each $[100]$ axis) between which the atom can move. This will give a mathe-

¹⁶ P. G. de Gennes, *Solid State Commun.* **1**, 132 (1963).

¹⁷ M. Tokunaga and T. Matsubara, *Progr. Theoret. Phys. (Kyoto)* **35**, 581 (1966).

¹⁸ M. Tokunaga, *Progr. Theoret. Phys. (Kyoto)* **36**, 857 (1966).

¹⁹ R. Brout, K. A. Müller, and H. Thomas, *Solid State Commun.* **4**, 507 (1966).

²⁰ L. Novakovic, *J. Phys. Chem. Solids* **27**, 1469 (1966).

²¹ H. Takahashi, *J. Phys. Soc. Japan* **16**, 1685 (1961).

mathematical complication, which we avoid for the present by simply assuming that the probability of tunneling between minima on different axes is negligible. Then the system is considered to be composed of three independent tunneling systems, where atoms move collinearly with the [100] direction and are tunneling between one pair of the three double minima lying along the ⟨100⟩ directions. Following Tokunaga and Matsubara,¹⁷ the effective Hamiltonian for the system where atoms are tunneling along the [001] direction is expressed as

$$H_{\text{eff}} = -2\Omega \sum_i S_i^x - \sum_{ik} J(\mathbf{R}_{ik}) S_i^x S_k^x, \quad (12)$$

where Ω is the kinetic energy of each atom and $J(\mathbf{R}_{ik})$ is the potential energy between atoms separated by \mathbf{R}_{ik} . The scattering cross section of neutrons is calculated by Tokunaga¹⁸ for the case when the energy width is small as compared with the characteristic energy of the tunneling motion. Since this condition is not satisfied in the critical temperature region, we have calculated the cross section in a self-consistent manner, using Green's function method. The details of the calculation will be reported in a separate paper. The preliminary result shows that the cross section is formally expressed as

$$\left(\frac{d^2\sigma}{d\Omega d\omega}\right)_{tn}^* = \frac{1}{3} N \frac{k'}{k} |F_{tn}(\mathbf{K})|^2 \frac{kT}{\pi \hbar^2} \times \frac{2\Omega \langle S^x \rangle 2\Gamma_{tn}}{(\omega^2 - \omega_1'^2)^2 + 4\Gamma_{tn}^2 \omega^2}, \quad (13)$$

$$\hbar\omega_1' = 2\Omega \left(1 - \frac{J(\mathbf{q})}{\Omega} \langle S^x \rangle - \frac{\Delta}{\Omega}\right)^{1/2}.$$

Here, ω_1' is the renormalized characteristic frequency of the collective tunneling mode; Δ and Γ_{tn} correspond to the shift and the damping constant of the mode, respectively; and $J(\mathbf{q})$ is the Fourier transform of $J(\mathbf{R})$. In this treatment, it is hard to give expressions for the parameters Δ and Γ_{tn} in terms of Ω and $J(\mathbf{R})$ explicitly. $F_{tn}(\mathbf{K})$ is the structure factor which is approximately given by

$$F_{tn}(\mathbf{K}) = \sum_j \mathbf{K} \cdot \Delta \mathbf{r}_j b_j e^{i\mathbf{K} \cdot \mathbf{r}_j}, \quad (14)$$

where $\Delta \mathbf{r}_j$ is the displacement vector of one of the potential minima on the [001] axis, for the j th atom ($\Delta \mathbf{r}_j \parallel [001]$). [In the derivation of Eqs. (13) and (14), we have neglected the contribution to the cross section from the "longitudinal" fluctuation, or $\langle S^x(t) S^x(0) \rangle$ -type correlation. This point will be discussed in Sec. V.] As there are three independent tunneling directions, the cross section from the whole system is given by the sum of expressions similar to Eq. (13) for the cases when $\Delta \mathbf{r} \parallel [100]$ and $\Delta \mathbf{r} \parallel [010]$.

For the overdamped case ($\Gamma_{tn} \gg 2\omega_1'$), we have the same expression as Eq. (10), viz., when \mathbf{q} is along ⟨100⟩ (see the Appendix),

$$\left(\frac{d^2\sigma}{d\Omega d\omega}\right)_{tn} = N \frac{k'}{k} \frac{|F_{tn}(\mathbf{K})|^2}{3\pi} \frac{kT}{\beta(T-T_0) + bq^2} \times \frac{\omega_1'^2 / 2\Gamma_{tn}}{\omega^2 + (\omega_1'^2 / 2\Gamma_{tn})^2}, \quad (15)$$

$$\beta = 2\pi N \mu^2 / C.$$

C is the Curie-Weiss constant, μ is the dipole moment per unit cell, and b is the coefficient of the quadratic term in the expansion of $J(\mathbf{q})$; $J(q) = J(0) + bq^2$. Equation (14) again coincides with Eq. (3) by equating

$$A = \beta/b, \\ \gamma = \omega_1'^2 / 2\Gamma_{tn}.$$

In this case, the parameter β can be calculated assuming that the dipole moment is given by the spontaneous polarization per unit cell. With the value of β thus calculated and the observed value of A , b is estimated to be 20.0 meV Å⁻². Again, we cannot obtain the value of ω_1' and Γ_{tn} separately from the observed value of γ .

The integrated intensity for this model is independent of Γ_{tn} and is calculated to be 6.8 b/sr at $T = 137^\circ\text{C}$ and $q = 0.12 \text{ \AA}^{-1}$, where the structure factor is estimated from Eq. (14) with the value of $\Delta \mathbf{r}_j$'s given by the equilibrium positions of the j th atom in the ferroelectric state.²²

As for the anisotropy of the intensity distribution in the \mathbf{q} space, it is explained qualitatively as follows. As is discussed in the Appendix, the integrated intensity in a general direction in the \mathbf{q} space is given by

$$\left(\frac{d\sigma}{d\Omega}\right)_{tn}^* = \frac{1}{6} N \frac{k'}{k} |F_{tn}(\mathbf{K})|^2 \times \frac{kT}{\beta(T-T_0) + 4\pi N \mu^2 \cos^2\phi + bq^2}, \quad (16)$$

where ϕ is the angle between \mathbf{q} and $\Delta \mathbf{r}_j$. The second term of the denominator is associated with the long-range electrostatic interaction included in $J(\mathbf{q})$. It is shown in the Appendix that

$$(\beta(T-T_0) + bq^2) / 4\pi N \mu^2 \approx 1/\epsilon(0).$$

Therefore, in the critical temperature region where $\epsilon(0) \cong 10^5$, the intensity is strongly ϕ -dependent and the direction of elongation of the intensity contour is along the ⟨100⟩ directions.

V. DISCUSSION

The quasielastic scattering of neutrons near the critical temperature in BaTiO₃ can be represented by

²² B. C. Frazer, H. R. Danner, and R. Pepinsky, Phys. Rev. **100**, 745 (1955).

the formula

$$\frac{d^2\sigma}{d\Omega d\omega} = \text{const} \frac{1}{A(T-T_0) + q^2\omega^2 + \gamma^2}.$$

This is in marked contrast to the case of SrTiO₃ and KTaO₃ in which a well-defined inelastic peak corresponding to the excitation of the soft-phonon mode was observed at temperatures very close to T_0 . We have demonstrated that the temperature dependence and the \mathbf{q} dependence of the quasi-elastic scattering can be explained equally well either by an overdamped phonon mode or by a tunneling mode.

The important characteristic of the critical scattering is its strong anisotropy in reciprocal space. If we take the phonon picture, this will be explained by the anisotropy in the characteristic frequency $\omega_1(\mathbf{q})$ and the damping constant $\Gamma'(\mathbf{q})$. On the other hand, if we accept the tunneling mode picture, it is attributed to the singularity of $J(\mathbf{q})$ around $\mathbf{q}=0$, as is discussed in the previous section.

It was previously reported⁶ that inelastic peaks due to excitation of a soft mode was observed at 230°C and 430°C. The frequencies were found to be much lower than those expected from Lyddane-Sachs-Teller relation. On the other hand, the line shapes do not seem to be broader than the instrumental resolution function. These experimental results are not explained by a simple overdamped mode model assuming Γ' is independent of ω , since the line shape of the soft mode should be considerably broader when the peak is shifted from the frequency of undamped mode. (See case B and case C of Fig. 8.) However, if we take into account a ω dependence in Γ , the sharp peaks observed at higher temperatures might be explained with the overdamped mode model as follows. We assume that the damping constant which describes the motion of the soft-mode phonon has a finite memory time and the time dependence of the damping constant is given by an exponential decay with a decay constant τ .¹⁴ The frequency spectrum of $\Gamma(\epsilon)$ is then given by

$$\Gamma(\omega) = \Gamma_0 / (1 - i\omega\tau).$$

With this spectrum for Γ , the neutron scattering cross section is expressed as

$$\left(\frac{d^2\sigma}{d\Omega d\omega} \right)_{dp} = N \frac{k'}{k} |F_{ph}(\mathbf{K})|^2 \frac{kT}{\pi} \frac{\bar{\Gamma}}{(\omega_1^2 - \omega^2\delta)^2 + \omega^2\bar{\Gamma}^2}, \quad (17)$$

$$\delta = 1 + \tau\Gamma_0 / (1 + \omega^2\tau^2),$$

$$\bar{\Gamma} = \Gamma_0 / (1 + \omega^2\tau^2).$$

The ω dependence of Eq. (17) is similar to a superposition of three Lorentzian peaks: One has a broad maximum at $\omega=0$ with an effective width of $\omega_1^2/\bar{\Gamma}$; the others are centered at $\pm\omega_1/\delta$ with effective widths of $\bar{\Gamma}/\delta$. It is possible to choose parameters τ and Γ_0 so that

the experimental line shapes as shown in Fig. 2 are qualitatively explained. However, at present it is difficult to assess the significance of these parameters.

Recently, the Raman scattering experiments in the tetragonal phase were performed by three groups. Among them, DiDomenico *et al.*¹⁵ observed a relaxation-type peak around $\omega=0$. They analyzed the data by the overdamped oscillator model and found $\Gamma/2\omega_1=1.15$ at 30°C. On the other hand, Pinczuk *et al.*²³ and Rimai *et al.*²⁴ observed a resonance-type Stokes line at room temperature with $\hbar\omega_1 \cong 0.6$ and 1.2 meV, respectively. The latter result is in line with the low estimate of the soft-mode energy shown in Fig. 1. Our result for the critical scattering seems to be closely related to the results due to DiDomenico *et al.*, though the half-width of the energy spectrum is appreciably different ($\Gamma/2\omega_1=4.6$ at 137°C as determined by neutron scattering).

In Tokunaga's treatment¹⁸ of the tunneling mode, the term proportional to $\langle S^z(t)S^z(0) \rangle$ -type correlation is explicitly taken into account, resulting in a relaxation-type correlation fluctuation. The experimental result, however, indicates that the observed relaxation-type fluctuation is not due to a $\langle S^z(t)S^z(0) \rangle$ -type correlation. Tokunaga has shown that the probability-density distribution contributing to this term is due to the overlap of the wave functions of the tunneling atoms and is symmetric with respect to the center of symmetry position, while the correlation $\langle S^z(t)S^z(0) \rangle$ is associated with the antisymmetric part. The form factor given in Eq. (14) is the Fourier transform of the antisymmetric part of the probability density. The observation of the intensity distribution around various reciprocal lattice points shows that the form factor is consistent with Eq. (14). For instance, in the intensity distribution around (200), the lobe elongated along [100] disappears because of the factor $(\mathbf{K} \cdot \Delta\mathbf{r})$ involved in Eq. (14). Therefore, we infer that the observed relaxation-type correlation fluctuation is not mainly due to $\langle S^z(t)S^z(0) \rangle$ -type correlation.

ACKNOWLEDGMENTS

We are indebted to M. Blume and H. J. Lee for developing the theoretical treatment on critical scattering and for conveying their results prior to publication. We also wish to thank B. C. Frazer, R. Nathans, and J. Skalyo for many stimulating discussions and V. Berluss for growing the excellent single crystal used in the present study.

APPENDIX

The integrated intensity of the critical scattering as calculated by a tunneling mode model is independent

²³ A. Pinczuk, W. Taylor, E. Burstein, and I. Lefkowitz, *Solid State Commun.* **5**, 429 (1967).

²⁴ L. Rimai, J. L. Parsons, J. T. Hickmott, and T. Nakamura, *Phys. Rev.* **168**, 623 (1968).

of Γ_{tn} and is given by

$$\left(\frac{d\sigma}{d\Omega}\right)_{tn}^z = \frac{1}{3}N |F_{tn}(\mathbf{K})|^2 \frac{2\Omega\langle S^z \rangle kT}{(\hbar\omega_1'(\mathbf{q}))^2}, \quad (\text{A1})$$

$$\hbar\omega_1'(\mathbf{q}) = 2\Omega(1 - J(\mathbf{q})/\Omega\langle S^z \rangle)^{1/2}.$$

To expand $J(\mathbf{q})$ in terms of \mathbf{q} , it should be noticed that $J(\mathbf{q})$ has a singularity at $\mathbf{q}=0$, due to the depolarization energy. This originates from the fact that the interaction energy which causes the tunneling fluctuation includes a long-range interaction; whence there exists a finite energy difference between the longitudinal fluctuation and the transverse fluctuation. This point has been discussed by Krivoglatz.²⁵ Taking out explicitly the term corresponding to the depolarization energy, we can expand $J(\mathbf{q})$ as

$$J(\mathbf{q}) = J(0) + 4\pi N\mu^2 \cos^2\phi + bq^2 + \dots, \quad (\text{A2})$$

where ϕ is the angle between the vectors \mathbf{q} and $[001]$, the direction of a tunneling motion. Then $[\hbar\omega_1'(\mathbf{q})]^2$ for small values of \mathbf{q} is expressed as

$$\hbar^2\omega_1'^2(\mathbf{q}) \cong \hbar^2\omega_1'^2(0) + 4\Omega\langle S^z \rangle 4\pi N\mu^2 \cos^2\phi + bq^2, \quad (\text{A3})$$

$$(\hbar\omega_1'(0))^2 = (2\Omega)^2[1 - J(0)/\Omega\langle S^z \rangle].$$

The energy $\hbar\omega_1'(0)$ is related to the static dielectric susceptibility, $\chi'(0)$, by the following equation:¹⁸

$$\chi'(0) = N\mu^2 2\Omega\langle S^z \rangle / (\hbar\omega_1'(0))^2. \quad (\text{A4})$$

On the other hand, $\chi'(0)$ is expressed by Curie-Weiss law as follows:

$$\chi'(0) \cong C/4\pi(T - T_0), \quad (\text{A5})$$

where C is the Curie-Weiss constant.

²⁵ H. A. Krivoglatz, Fiz. Tverd. Tela 5, 3439 (1963) [English transl.: Soviet Phys.—Solid State 5, 2526 (1964)].

By substituting Eqs. (A3), (A4), and (A5) into (A1), we have

$$\left(\frac{d\sigma}{d\Omega}\right)_{tn}^z = \frac{1}{3}N |F_{tn}(\mathbf{K})|^2 \frac{1}{2\beta(T - T_0) + 4\pi N\mu^2 \cos^2\phi + bq^2} \frac{kT}{\beta = 2\pi N\mu^2/C}. \quad (\text{A6})$$

For the special cases when \mathbf{q} is taken perpendicular and parallel to the direction of the tunneling motion, $\Delta\mathbf{r}$, we have

$$\left(\frac{d\sigma}{d\Omega}\right)_{tn}^z = \frac{1}{3}N |F_{tn}(\mathbf{K})|^2 \frac{1}{2\beta(T - T_0) + bq^2} \frac{kT}{q \perp \Delta\mathbf{r}}, \quad (\text{A7})$$

$$\left(\frac{d\sigma}{d\Omega}\right)_{tn}^z = \frac{1}{3}N |F_{tn}(\mathbf{K})|^2 \frac{1}{2\beta(T - T_0) + 4\pi N\mu^2 + bq^2} \frac{kT}{\mathbf{q} \parallel \Delta\mathbf{r}}. \quad (\text{A7}')$$

Equation (A7) corresponds to the cross section due to a transverse fluctuation while Eq. (A7') is the cross section due to a longitudinal fluctuation. The cross section due to the longitudinal fluctuation is negligibly small as compared with the cross section due to the transverse fluctuation in the critical temperature range. This can be seen as follows. From Eq. (A5), $\chi'(0)$ is given in terms of β as

$$\chi'(0) = N\mu^2/2\beta(T - T_0).$$

Since the value of bq^2 is of the same order of magnitude as $\beta(T - T_0)$ in the temperature range and \mathbf{q} range under investigation, we have

$$(\beta(T - T_0) + bq^2)/4\pi N\mu^2 \approx 1/4\pi\chi_{(0)} \cong 1/\epsilon_{(0)}.$$

Therefore, in the critical temperature region where $\epsilon(0) \gtrsim 10^4$, we can neglect the contribution from longitudinal fluctuation. By summing up the contribution due to three independent tunneling motions, we have the following expression for the integrated cross section when \mathbf{q} is taken along $\langle 100 \rangle$ directions:

$$\left(\frac{d\sigma}{d\Omega}\right)_{tn}^z = \frac{1}{3}N |F_{tn}(\mathbf{K})|^2 \frac{1}{2\beta(T - T_0) + bq^2} \frac{kT}{\beta}. \quad (\text{A8})$$